



UNIVERSITY OF LEEDS

This is a repository copy of *Experimental Modeling of Flavonoid-Biomembrane Interactions*.

White Rose Research Online URL for this paper:  
<http://eprints.whiterose.ac.uk/109966/>

Version: Accepted Version

---

**Article:**

Sanver, D, Murray, BS [orcid.org/0000-0002-6493-1547](https://orcid.org/0000-0002-6493-1547), Sadeghpour, A et al. (2 more authors) (2016) *Experimental Modeling of Flavonoid-Biomembrane Interactions*. *Langmuir*, 32 (49). pp. 13234-13243. ISSN 0743-7463

<https://doi.org/10.1021/acs.langmuir.6b02219>

---

© 2016 American Chemical Society. This document is the Accepted Manuscript version of a Published Work that appeared in final form in *Langmuir*, copyright © American Chemical Society after peer review and technical editing by the publisher. To access the final edited and published work see <https://doi.org/10.1021/acs.langmuir.6b02219>.

**Reuse**

Unless indicated otherwise, fulltext items are protected by copyright with all rights reserved. The copyright exception in section 29 of the Copyright, Designs and Patents Act 1988 allows the making of a single copy solely for the purpose of non-commercial research or private study within the limits of fair dealing. The publisher or other rights-holder may allow further reproduction and re-use of this version - refer to the White Rose Research Online record for this item. Where records identify the publisher as the copyright holder, users can verify any specific terms of use on the publisher's website.

**Takedown**

If you consider content in White Rose Research Online to be in breach of UK law, please notify us by emailing [eprints@whiterose.ac.uk](mailto:eprints@whiterose.ac.uk) including the URL of the record and the reason for the withdrawal request.



[eprints@whiterose.ac.uk](mailto:eprints@whiterose.ac.uk)  
<https://eprints.whiterose.ac.uk/>

This document is confidential and is proprietary to the American Chemical Society and its authors. Do not copy or disclose without written permission. If you have received this item in error, notify the sender and delete all copies.

### Experimental Modelling of Flavonoid-Biomembrane Interactions

Journal:	<i>Langmuir</i>
Manuscript ID	la-2016-022194.R1
Manuscript Type:	Article
Date Submitted by the Author:	n/a
Complete List of Authors:	Sanver , Didem ; The University of Leeds, Chemistry Murray, Brent; University of Leeds, School of Food Science & Nutrition Sadeghpour, Amin; University of Leeds, School of Food Science & Nutrition Rappolt, Michael; University of Leeds , Nelson, Andrew; University of Leeds, School of Chemistry

SCHOLARONE™  
Manuscripts

# Experimental Modelling of Flavonoid-Biomembrane Interactions

*Didem Sanver<sup>†,‡</sup>, Brent S. Murray<sup>†,\*</sup>, Amin Sadeghpour<sup>†</sup>, Michael Rappolt<sup>†</sup>, Andrew L. Nelson<sup>§</sup>*

<sup>†</sup>School of Food Science and Nutrition, and <sup>§</sup>School of Chemistry, University of Leeds, Leeds

LS2 9JT, UK

<sup>‡</sup>Department of Food Engineering, Necmettin Erbakan University, Koycegiz Kampusu, 420701

Konya, Turkey

Flavonoid, Interaction, DOPC, Biomembrane Model, Rapid Cyclic Voltammetry, Langmuir trough, BAM, SAXS

1 **ABSTRACT:** Non-specific interactions of flavonoids with lipids can alter the membrane's  
2 features (e.g. thickness and fluctuations) as well as influence their therapeutic potentials.  
3 However, relatively little is known about the details of how flavonoids interact with lipid  
4 components. Structure-dependent interactions of a variety of flavonoids with phospholipid  
5 monolayers on a mercury (Hg) film electrode were established by rapid cyclic voltammetry  
6 (RCV). The data revealed that flavonoids adopting a planar configuration altered the membrane  
7 properties more significantly than non-planar flavonoids. Quercetin, rutin and tiliroside were  
8 selected for follow-up experiments with Langmuir monolayers, Brewster Angle Microscopy  
9 (BAM) and small angle X-ray scattering (SAXS). Relaxation phenomena in DOPC monolayers  
10 and visualization of the surface with BAM revealed a pronounced monolayer stabilization effect  
11 with both quercetin and tiliroside, whereas rutin disrupted the monolayer structure rendering the  
12 surface entirely smooth. SAXS showed a monotonous membrane thinning for all compounds  
13 studied associated with an increase in the root mean square fluctuations of the membrane. Rutin,  
14 quercetin and tiliroside decreased the bilayer thickness of DOPC by  $\sim 0.45$  Å,  $0.8$  Å, and  $1.1$  Å at  
15 6 mol %, respectively. In addition to the novelty of using lipid monolayers to systematically  
16 characterize the structure activity relationship (SAR) of a variety of flavonoids; this is the first  
17 report investigating the effect of tiliroside with biomimetic membrane models. All the flavonoids  
18 studied are believed to be localized in the lipid/water interface region. Both this localization and  
19 the membrane perturbations have implications for their therapeutic activity.

### Introduction

Flavonoids are of great importance due to their potential anti-oxidative, anti-inflammatory and immune regulatory actions and many epidemiologic studies show a relationship between flavonoid consumption in the diet and reduced risk of several chronic diseases, including cancer and diabetes.<sup>1,2,3</sup> Quercetin, one of the most widely studied flavonoids, has been claimed to be a better mast cell stabilizer than Cromolyn which is the only related pharmaceutical available on the market.<sup>4</sup> Quercetin was found to regulate allergic reactions by limiting the release of mediators that trigger allergy, such as histamine, prostaglandin DS (PGD<sub>2</sub>), tumor necrosis factor (TNF) and several cytokines like IL-8.<sup>4</sup> Similarly, rutin, a glycoside of quercetin, was demonstrated to serve as an anti-inflammatory agent in the treatment of osteoarthritis, as monitored via the decrease in the serum level of a type II collagen biomarker, Coll2-1.<sup>5</sup>

The molecular mechanism of action of flavonoids is a longstanding debate. Although their mechanism has been widely attributed to specific interactions involving protein-flavonoid binding, recent studies have intimated that flavonoids alter biomembrane organization which might then lead to modifications in membrane protein function.<sup>6,7,8</sup> The simplest techniques which can be used to test this hypothesis involve the use of biological membrane models with associated biophysical techniques. The advantages of these systems arise from their reduced complexity and improved experimental control compared to cell cultures.<sup>9,10</sup>

In spite of the work done looking at the biological activity of flavonoids, the interaction mechanism between flavonoids and model biological membranes has not yet been fully understood and the literature so far remains controversial. Flavonoid concentration and lipid

1  
2  
3 1 membrane composition as well as the diversity of techniques employed could contribute to the  
4  
5 2 variation of the results.<sup>11</sup>  
6  
7

8 3 One motivation of this study was to use a very well characterized system to avoid the influence  
9  
10 4 of an additional variable involved in flavonoid-membrane interactions. For this reason, we have  
11  
12 5 excluded cholesterol as many other authors have done<sup>6</sup>. Hence, unlike many conventional  
13  
14 6 membrane models of liposome bilayers, this study aimed to use monolayer membrane models in  
15  
16 7 proof of concept experiments with one lipid type; 1,2 dioleoyl-*sn*-glycero-3-phosphocholine  
17  
18 8 (DOPC) to screen flavonoid interactions. For this, a number of techniques including an *on-line*  
19  
20 9 high-throughput sensing system, custom designed for biomembrane interactions, were applied.<sup>12</sup>  
21  
22 10 This system is based on an electrochemical membrane model consisting of a DOPC monolayer  
23  
24 11 coated mercury (Hg) electrode and rapid cyclic voltammetry (RCV), which allows rapid  
25  
26 12 screening of large numbers of compounds and has been extensively used by other workers in the  
27  
28 13 area.<sup>13,14,15</sup>  
29  
30  
31  
32  
33

34 14 Although this sensing device was previously used to screen a number of membrane active  
35  
36 15 compounds from toxins to drugs, the current work aimed to reinforce the sensing system for food  
37  
38 16 ingredients for the first time. A successful application of such a sensing system can rapidly  
39  
40 17 establish a structure activity relationship of a variety of food compounds with membranes.  
41  
42

43 18 Subsequent to the initial RCV screening, selected flavonoids were studied via classic spread  
44  
45 19 Langmuir monolayers at the air-water (A-W) interface. The aim of using such a conventional  
46  
47 20 method with free-standing monolayers was to correlate the interactions observed on the DOPC  
48  
49 21 adsorbed Hg electrode. Moreover, Langmuir monolayers are excellent systems to monitor film  
50  
51 22 stability. Such information is especially useful in investigation of the therapeutic effects of  
52  
53 23 flavonoids. As far as we are aware, the interaction of only one flavonoid, quercetin, with  
54  
55  
56  
57  
58  
59  
60

1 phospholipid monolayers has been studied in detail previously,<sup>39</sup> whereas in this study a range of  
2 flavonoids have been studied. Surface pressure ( $\pi$ ) versus area per molecule ( $\text{\AA}$ ) isotherms  
3 facilitated study of the adsorption and penetration of the flavonoids on and into DOPC  
4 monolayers. In addition, a direct observation of the monolayer stability in the absence and  
5 presence of the test compounds was made by measuring the desorption rate of the spread  
6 monolayers at constant surface pressure.<sup>16</sup> The adsorption and stability behavior of the  
7 monolayers was also studied by Brewster Angle Microscopy (BAM).

8 Finally, characterization of flavonoid lipid interactions was achieved using phospholipid  
9 vesicles, a step up in complexity from monolayers. Small angle X-ray scattering (SAXS) was  
10 performed to quantitatively analyze the interactions between flavonoids and lipid multilamellar  
11 vesicles (MLVs) in terms of alterations in (i) lattice spacing, (ii) membrane thickness, (iii) water  
12 layer thickness, and (iv) positional membrane fluctuations.

13 All three model systems above used DOPC as the lipid component for several reasons. The  
14 fluid nature of DOPC is highly compatible with fluid Hg, which allows the spread monolayer to  
15 be defect-free and self-sealing.<sup>17</sup> Furthermore, DOPC MLVs are the most preferred systems for  
16 SAXS studies since they produce a stable lamellar ( $L\alpha$ ) phase which is ubiquitous in real  
17 biological membranes, unlike non-lamellar lipids.<sup>18,19</sup>

18 To the best of our knowledge, this is the first systematic study investigating both monolayers  
19 and bilayers for interactions of a wide range of flavonoids with biomembrane models. A  
20 consensual view was derived from the data using a `cross platform` approach via distinctly  
21 varying techniques which give complementary information on the physical, chemical mechanism  
22 of interactions. A range of flavonoids (Figure 1) with significantly different structures was

1 selected for study based on: the existence of double bond in the ring C, the degree of  
2 hydroxylation and the presence of sugar group moiety.

### 3 **Experimental Methods**

#### 4 **Materials**

5 DOPC with the purity of > 99% was purchased from Avanti Polar Lipids (USA). The  
6 flavonoids quercetin dihydrate, rutin trihydrate (quercetin-3- $\beta$ -D-rutinoside), naringenin,  
7 hesperetin, (+) - catechin hydrate and naringin were supplied by Sigma-Aldrich (Germany).  
8 Kaempferol and tiliroside were obtained from Extrasynthese (France). Phosphate buffered saline  
9 (PBS) powder was used to prepare the pH 7.4 buffer solution, and was obtained from Sigma-  
10 Aldrich. For monolayer studies, one batch of PBS was dissolved in one liter of Milli-Q water  
11 (Millipore Inc.,  $\Omega = 18.2 \text{ M}\Omega\cdot\text{cm}$ ) to give 0.01 M phosphate,  $0.138 \text{ mol dm}^{-3} \text{ NaCl} + 0.0027 \text{ mol}$   
12  $\text{dm}^{-3} \text{ KCl}$ . Ethanol (absolute, AR, Merck) and dichloromethane (anhydrous,  $\geq 99.8\%$ , Sigma-  
13 Aldrich) were used as received without further purification. A flavonoid concentration of 10  
14  $\mu\text{mol dm}^{-3}$  was chosen for monolayer studies as it is in the range of physiological uptake  
15 concentrations in body<sup>20</sup> and a dose-dependent response was investigated in this range via RCV.

#### 16 **Electrochemical measurements**

17 A stock solution of flavonoids dissolved in ethanol and a stock solution of DOPC ( $2 \text{ mg ml}^{-1}$ )  
18 in PBS buffer were freshly prepared prior to experiments.

19 The microfabricated platinum (Pt) electrodes (MPE) (Tyndall National Institute, Ireland) were  
20 composed of eight 0.48 mm radius discs and used as working electrodes. Their cleaning  
21 procedure has been previously described in detail.<sup>12</sup> Electrodeposition of Hg on Pt electrode was  
22 performed in a standard three electrode cell that contains Ag/AgCl,  $3.5 \text{ mol dm}^{-3} \text{ KCl}$  as  
23 reference electrode and platinum rod as a counter electrode. Electrodes were connected to an

1  
2  
3 1 Autolab PGSTAT 30 potentiostat (Eco Chemie, Utrecht, Netherlands) interfaced to a PowerLab  
4  
5 2 4/25 signal generator (AD Instruments Ltd.) monitored by Scope™ software. Current vs.  
6  
7  
8 3 potential RCV scans were recorded via the software at a scan rate of 40 Vs<sup>-1</sup>. Prior to lipid  
9  
10 4 deposition, the surface of Hg is cleaned in situ by flushing the system with PBS buffer at the  
11  
12 5 voltage of ~ -3.0 V and 100-200 μL of the lipid solution was injected into the system at the same  
13  
14 6 voltage, as described previously<sup>15</sup>. After obtaining a stable DOPC monolayer on Hg, the  
15  
16 7 flavonoids from the stock solutions were introduced into the flow cell at the predetermined  
17  
18 8 concentrations and alterations in the monolayer were monitored by RCV with a total sampling  
19  
20 9 time of 5 minutes by cycling the potential from -0.4 to -1.2 V. The ethanol concentration did not  
21  
22 10 exceed 1 % in the final solution and all controls in this study refer to the control with exposed  
23  
24  
25 11 ethanol alone.  
26  
27  
28

## 29 12 **Surface pressure-area isotherms of Langmuir monolayers**

30  
31  
32 13 A specialist *in-house* Langmuir film balance featuring a rhomboidal shape PTFE barrier whose  
33  
34 14 set up was described in detail previously,<sup>21</sup> was used throughout this work. The surface  
35  
36 15 pressure-area ( $\pi$ - $A$ ) isotherms were produced by a Wilhelmy plate of roughened mica (~3 cm)  
37  
38 16 which was dipped into the subphase at the center of the trough.  
39  
40

41 17 A lipid solution of DOPC was prepared in an ethanol : dichloromethane mixture at the ratio of  
42  
43 18 1:9. A monolayer was obtained by spreading DOPC solution (0.2 mg/mL) over the subphase of  
44  
45 19 PBS buffer (pH, 7.4). Following solvent evaporation for 15 minutes, the monolayer was slowly  
46  
47 20 compressed at the rate of 8.6 mm<sup>2</sup> s<sup>-1</sup> (corresponding to 3.6 Å<sup>2</sup> min<sup>-1</sup>), starting from an initial  
48  
49 21 (maximum) through area of 22 500 mm<sup>2</sup>. This compression rate is considered to be slow enough  
50  
51 22 to represent the “true equilibrium” isotherm since decreasing the compression rate further created  
52  
53 23 no difference in the  $\pi$ - $A$  isotherms. The monolayer was compressed to  $\pi = 30$  mN m<sup>-1</sup>, which  
54  
55  
56  
57  
58  
59  
60

1 corresponds to a typical biological membrane pressure,<sup>22</sup> and flavonoids were injected beneath  
2 the monolayer to give a final subphase concentration of  $10 \mu\text{mol dm}^{-3}$ . The system was then  
3 allowed to stabilize for around 20 minutes after flavonoid injection and the film stability was  
4 monitored as a function of the change in the trough area by maintaining the pressure constant at  
5  $30 \text{ mN m}^{-1}$  for one hour. Measurement of area loss at  $\pi = 30 \text{ mN m}^{-1}$  was detected for DOPC  
6 monolayer alone and in the presence of flavonoids by extrapolating the trough area ( $A$ ) at time  $t$ ,  
7 relative to the initial starting area ( $A_o$ ), i.e.  $A/A_o$ , as a function of time.

8 At the end of 1 h, the monolayer was expanded to its maximum area and recompressed to the  
9 collapse point. Recompression was done to observe any changes in the  $\pi$ - $A$  isotherm indicative  
10 of flavonoid-monolayer interactions.

### 11 **Brewster Angle Microscopy (BAM)**

12 Brewster Angle Microscopy is a widely used technique for studying thin film structure on  
13 liquid surfaces. The BAM system and its operation described in detail elsewhere<sup>23</sup> and only brief  
14 details are presented here. A *BAM2plus* Brewster Angle Microscope (NFT, Gottingen,  
15 Germany), combined with the Langmuir trough above was employed to visualize the  
16 morphology of the DOPC monolayers before and after flavonoid addition. The laser output  
17 power was kept constant at 18% for all experiments and the shutter speed for the camera was  
18 fixed at  $1/50 \text{ s}$  at the Brewster angle of  $53.15^\circ$  for the pure A-W interface. The analyzer and  
19 polarizer angles were set to zero. Since there is no p-polarized reflection from pure water at the  
20 Brewster angle, in principle BAM only records the reflected intensity arising from the surface  
21 film at the interface. Although the lateral resolution of the BAM2 images is considerably less  
22 ( $\sim 2 \mu\text{m}$ ) compared to fluorescence microscopy, its advantage arises from being a completely  
23 non-invasive technique without requiring sample labelling.<sup>24</sup>

1  
2  
3  
4  
5  
6  
7  
8  
9  
10  
11  
12  
13  
14  
15  
16  
17  
18  
19  
20  
21  
22  
23  
24  
25  
26  
27  
28  
29  
30  
31  
32  
33  
34  
35  
36  
37  
38  
39  
40  
41  
42  
43  
44  
45  
46  
47  
48  
49  
50  
51  
52  
53  
54  
55  
56  
57  
58  
59  
60

1



1  
2  
3 described previously in depth<sup>27,28</sup> – for reviews see Rappolt et al.<sup>29</sup> and Pabst et al.<sup>30</sup> The bilayer  
4  
5  
6 model used to interpret the data and its applications have also been described previously.<sup>31</sup>  
7  
8 Lamellar repeat distance  $d$  and the head-to-head group thickness,  $d_{\text{HH}}$  were directly obtained  
9  
10 from the fits to the scattered intensities  $I = S(q)|F(q)|^2/q^2$ , ( $S(q)$  = structure factor;  $F(q)$  = form  
11  
12 factor). Mean square fluctuations of the membrane position,  $\sigma$  were derived from the Caillé  
13  
14 parameter,  $\eta$ ,  
15  
16

$$17 \quad \sigma = \sqrt{\eta} \frac{d}{\pi} \quad (1)$$

18  
19  
20 where  $d$ , is the lamellar repeat distance.  
21  
22  
23  
24  
25  
26  
27  
28  
29  
30  
31  
32  
33  
34  
35  
36  
37  
38  
39  
40  
41  
42  
43  
44  
45  
46  
47  
48  
49  
50  
51  
52  
53  
54  
55  
56  
57  
58  
59  
60

## 1       **Results and Discussion**

### 2       **Electrochemical Screening of flavonoid-DOPC interactions**

3       RCV plots for the DOPC monolayers with and without flavonoid at the studied concentrations  
4       are presented in **Figure 2**. It can clearly be seen that introduction of some compounds leads to a  
5       significant change in the current versus voltage plot. An alteration in the peak height, position  
6       and shape of the current peaks results in a “finger-print” RCV profile for each class of  
7       compounds. In RCV measurements with a DOPC coated electrode, suppression of the  
8       capacitance current peaks with little effect on the capacitance current baseline is representative  
9       of species adsorbing on the monolayer surface. A clear increase in the baseline capacitance  
10      current with depression of the capacitance peaks shows a penetration or disruption of the layer  
11      by compounds since the low dielectric constant of the monolayer's apolar core is disturbed.<sup>32</sup>

12      At the concentrations of  $10 \mu\text{mol dm}^{-3}$  (red line in **Figure 2**), the most significant changes in  
13      DOPC properties following introduction of flavonoids were seen with quercetin and kaempferol  
14      represented as a total capacitance peak current suppression and an increase in capacitance  
15      baseline height. Tiliroside showed a smaller effect; naringenin, hesperetin and catechin displayed  
16      an apparently even weaker interaction with DOPC – displayed as an intermediate capacitance  
17      peak current suppression and rutin and naringin apparently displayed no significant interaction  
18      with DOPC at all. The increase in baseline capacitance current following quercetin and  
19      kaempferol addition is strong evidence that these compounds penetrated the DOPC layer  
20      whereas the remaining compounds probably remained adsorbed on the surface.

21      The effect of flavonoids was found to be concentration dependent; at increased concentrations  
22      of  $35 \mu\text{mol dm}^{-3}$  (blue line-**Figure 2**), majority of the compounds revealed a more pronounced

1  
2  
3 1 effect. A slight response was even observed with rutin at this concentration along with an  
4  
5  
6 2 indistinct hump formation on the baseline, but naringin still displayed no interaction.

7  
8 3 The results above suggest that the interactions are directly related to the compound structure,  
9  
10 4 especially to their conformations. Quercetin and kaempferol show the strongest interaction with  
11  
12 5 significant penetration of the DOPC monolayer and they possess two coplanar rings whereas the  
13  
14 6 third ring is oriented at right angles. Presumably the planar two rings facilitate the interaction and  
15  
16 7 penetration of the compound within the membrane. However, even such strong interactions were  
17  
18 8 found to be reversible and DOPC membrane could be recovered, indicating flavonoids do not  
19  
20 9 replace or destabilize the membrane.

21  
22  
23  
24 10 The insignificant interactions of rutin and naringin with DOPC could be related to the two  
25  
26 11 glycoside groups attached to quercetin and naringenin, respectively, which sterically hinder any  
27  
28 12 significant interaction. Compounds showing intermediate interaction with and no penetration of  
29  
30 13 the DOPC monolayer include naringenin, hesperetin and catechin. Each of these compounds has  
31  
32 14 the common structural characteristic where the second ring of the two-ringed structure is kinked,  
33  
34 15 which might hinder interaction. Tiliroside is a more bulky molecule and exhibits a stronger  
35  
36 16 interaction than the other three molecules. Tiliroside has one glycoside group positioned between  
37  
38 17 the flavonoid moiety and a further ring but the flavonoid group contains the two ringed planar  
39  
40 18 moiety which could account for the stronger interaction as with quercetin and kaempferol.

41  
42  
43  
44 19 Detection limits in terms of the minimum concentrations of the compounds which exerted a  
45  
46 20 significant effect on the monolayer structural properties were calculated based on the RCV  
47  
48 21 measurements. The first current peak was used in estimation of the limit of detection (LOD) and  
49  
50 22 a detailed procedure for LOD calculation has been described previously.<sup>33</sup> A rank order of the  
51  
52 23 LOD values is displayed in **Table 1**. These follow the general order of compound interaction as

1 described in the paragraph above. Furthermore the estimated LOD values are plotted against the  
2 corresponding log octanol-water partition coefficients ( $\log P$ ) are shown in **Figure 3**. The  $\log P$   
3 value has been widely used to characterize the hydrophobicity of molecules and the tendency for  
4 flavonoids to interact with bio-mimetic membranes.<sup>11</sup> However, it can clearly be seen from  
5 **Figure 3** that there is no systematic correlation between the LOD value and  $\log P$ . The finding  
6 that flavonoid structure is the critical factor in determining its interaction with phospholipid  
7 membranes is commensurate with other studies, suggesting that in the presence of molecules of  
8 comparable hydrophobicity, the detailed structural properties of the molecules need to be  
9 carefully taken into consideration.<sup>33,11,34</sup>

10 It is interesting to put these results in the context of those from other studies. Previous studies  
11 confirm that the existence of a C2-C3 double bond in the structure of quercetin and kaempferol  
12 renders these compounds more planar<sup>35</sup> and consequently results in stronger interactions with  
13 membrane components, compared to the non-planar configurations of naringenin and  
14 hesperetin.<sup>34</sup> One of the very first studies comparing membrane interactions of quercetin, rutin,  
15 naringenin and hesperetin with DPPC liposomes, using differential scanning calorimetry (DSC),  
16 revealed that the strongest flavonoid-DPPC interaction were observed with quercetin.<sup>36</sup> These  
17 findings were supported by further studies,<sup>34</sup> investigating the affinity of a set of flavonoids,  
18 including quercetin and naringenin, towards artificial vesicles via fluorescence quenching of the  
19 membrane probe 1,6-diphenyl-1,3,5-hexa-triene (DPH). Quercetin was found to have a higher  
20 membrane affinity compared to naringenin. Both studies attributed such a response to quercetin's  
21 planar structure, and proposed that the tilted configuration of naringenin and hesperetin rendered  
22 them less likely intercalate into the ordered structures of the packed phospholipid layers.<sup>34</sup>

1 The effect of glycoside moieties in hindering flavonoid/lipid membrane interaction has been  
2 observed elsewhere. The disaccharide moiety of rutin hinders its ability to interact with DPPC  
3 bilayers by rendering the molecule less hydrophobic.<sup>36</sup> Similarly, hesperetin (HT) was found to  
4 be more interactive with DMPC liposomes than its glucoside hesperidin (HD).<sup>37</sup> Biophysical  
5 studies in conjunction with human studies reported that absorption of aglycones was not only  
6 faster but also in five times greater than their glucoside forms.<sup>38</sup>

### 7 **Interactions of selected flavonoids with air-water monolayers of DOPC**

8 On the basis of the RCV results, the aglycone (i.e., without the sugar) quercetin, and two  
9 glycosides - tiliroside (one sugar moiety in the structure) and rutin (two sugar moieties in the  
10 structure), were selected for follow-up experiments with Langmuir monolayers, since they  
11 appeared to exhibit particularly representative effects of varying degrees of interaction.

12 As seen in **Figure 4a**, the introduction of quercetin ( $10 \mu\text{mol dm}^{-3}$ ) into the subphase did not  
13 provoke an immediate increase in the monolayer area at low surface pressures (below  $5 \text{ mN m}^{-1}$ ).  
14 However, the monolayer exhibited a more expanded isotherm when the pressure was increased  
15 further. The isotherm shifted towards a larger area per (DOPC) molecule ( $\sim 67 \text{ \AA}^2$ ) compared to  
16 that of the pure DOPC monolayer ( $\sim 60 \text{ \AA}^2$ ) at a surface pressure of  $30 \text{ mN m}^{-1}$ . It is assumed  
17 this shift occurred due to the area occupied by quercetin molecules inserted into the monolayer,  
18 and is observed all along the isotherm, indicating that the molecule remained in the monolayer  
19 at even higher surface pressures. This result is in agreement with the only other study of  
20 quercetin interacting with Langmuir monolayers of phospholipid (DPPC), published recently.<sup>39</sup>  
21 Similar to the present findings, the authors reported an increase in surface pressure due to the  
22 effective incorporation of molecule into the model lipid membrane.<sup>39</sup> In the same study, a  $\pi$ - $A$   
23 isotherm for pure quercetin spread on the air/water interface was also produced with a maximum

1 surface pressure of just above  $20 \text{ mN m}^{-1}$  before the collapse.<sup>39</sup> Based on the area per quercetin  
2 molecule ( $A_{flav} = 89 \text{ \AA}^2$ ) at  $\pi = 20 \text{ mN m}^{-1}$ , taken from this study, we attempted to quantify the  
3 amount of adsorption of quercetin into the DOPC monolayers, assuming ideal mixing. In other  
4 words, the mole fraction of quercetin ( $f_{flav}$ ) in the mixture was calculated via:

$$A_{total} = (1-f_{flav}) A_{lipid} + f_{flav} * A_{flav} \quad (2)$$

5 :where,  $A_{total}$  ( $78 \text{ \AA}^2$ ),  $A_{lipid}$  ( $72 \text{ \AA}^2$ ) and  $A_{flav}$  ( $89 \text{ \AA}^2$ ) signify the area per molecule in the mixed  
6 monolayer, area per lipid molecule and area per quercetin molecule, respectively. In the current  
7 study,  $f_{flav}$  was found as around 35% which shows a high passive adsorption of quercetin  
8 molecule into DOPC monolayers.

9  
10 **Figure 4b** shows the compression isotherm of DOPC monolayer in the presence of tiliroside  
11 ( $10 \mu\text{mol dm}^{-3}$ ). Unlike quercetin, tiliroside injection at a surface pressure of  $30 \text{ mN m}^{-1}$  caused a  
12 very distinct increase in the molecular area of the DOPC monolayer at low surface pressures  
13 only. On compression to higher surface pressures, a decrease in the molecular area is observed,  
14 suggesting molecules being expelled from the film.

15 At first glance, **Figure 4c** suggests no significant effect of rutin injected beneath DOPC  
16 monolayers, implying there is no definitive interaction. However, further surface characterization  
17 via BAM indicated significant effects of this compound on the monolayer (see later). A recent  
18 study pointed to a similar behavior of pure DOPC monolayers in the presence of the cationic  
19 photosensitizer methylene blue (MB)<sup>40</sup>, that has almost the same  $\log P$ <sup>41</sup> as rutin ( $\sim -0.9$ ).  
20 Although, the surface pressure of DOPC remained unaltered with MB incorporation, further  
21 analysis using polarization-modulated infrared reflection-absorption spectroscopy (PM-IRRAS)  
22 revealed the adsorption of MB *onto* the polar surface which then further leads its binding close to  
23 the double bonds of the hydrophobic chains.

1  
2  
3 1 Film loss and hence contraction of the spread monolayer films is inevitable when monolayers  
4  
5 2 are maintained at a constant surface pressure lower than the equilibrium spreading pressure ( $\pi <$   
6  
7  
8 3  $\pi_e$ ) over a certain period of time.<sup>42</sup>  $\pi_e$  is the maximum surface pressure ( $\pi_{eDOPC} = 46.1 \text{ mN m}^{-1}$ )  
9  
10 4 which monolayers can be compressed to before they collapse. Relaxation of the spread films  
11  
12 5 arises from desorption of molecules into the bulk phase at  $\pi$  values lower than  $\pi_e$ .<sup>43</sup> This  
13  
14 6 phenomenon gives information about the film stability. The effect of flavonoids on the molecular  
15  
16 7 area relaxation for DOPC monolayers is demonstrated in **Figure 5** at a constant  $\pi$  of  $30 \text{ mN m}^{-1}$ .  
17  
18 8 The change in area  $A$ , relative to the maximum area  $A_0$ , was monitored as a function of time,  $t$ .  
19  
20 9 Here, note that the saw-tooth appearance on **Figure 5** is due to the discrete time step between  
21  
22 10 alterations of the barrier position to maintain constant  $\pi = 30 \text{ mN m}^{-1}$ . The striking membrane-  
23  
24 11 stabilizing action of quercetin, suggesting lack of phospholipid desorption from the monolayer, is  
25  
26  
27 12 observed in **Figure 5a**. A similar stabilizing effect was observed also with tiliroside **Figure 5b**.  
28  
29  
30

31  
32 13 Membrane stabilization is an important phenomenon since it is believed to be a key  
33  
34 14 mechanism by which many drugs exert their beneficial effects. A recent study indicated  
35  
36 15 quercetin as a better mast cell 'stabilizer' than Cromolyn, which is the only drug available on the  
37  
38 16 market.<sup>4</sup> Moreover, molecular dynamics simulations, NMR and imaging techniques were used to  
39  
40 17 probe the membrane stabilizing effect of quercetin on DPPC bilayers<sup>44</sup> and quercetin was found  
41  
42 18 to bind to the membrane surface via hydrogen bonds at the lipid/water interface.<sup>44</sup> Apart from  
43  
44 19 quercetin, some other flavonoids have also been reported to exhibit stabilizing or destabilizing  
45  
46 20 effects. Such observations were made with milk thistle flavonoids: silybin and  
47  
48 21 dihydroxyquercetin (taxifolin). Dihydroxyquercetin stabilized the membranes whilst silybin  
49  
50 22 destabilized the lipid layers.<sup>45</sup>  
51  
52  
53  
54  
55  
56  
57  
58  
59  
60

## 1       **Topographical Characteristics of DOPC monolayers**

2       In agreement with previous studies,<sup>46,47</sup> pure DOPC monolayers formed 2D foam-like  
3       structures with circular shapes and small domains within their interior at very low surface  
4       pressures (data is not shown). All these structures disappeared during monolayer compression  
5       and no visible features were seen up to the collapse point ( $\sim\pi = 40$ ), giving a homogeneous liquid  
6       expanded phase only. A few bright features were formed and flickered at the collapse point,  
7       which is assumed to be an indication of multilayer formation.<sup>48</sup> These low density of bright  
8       ‘crystallites’ were observed with quercetin and tiliroside throughout the compression. Rutin,  
9       however, did not alter the observed morphology of the DOPC monolayer.

10       The images in **Figure 6** illustrate the monolayer structure after the monolayer had been fully  
11       compressed to the collapse pressure ( $\pi = \sim 41 \text{ mN m}^{-1}$ ). **Figure 6a** shows the formation of large  
12       lipid domains with pure DOPC. Although the molecular mechanism behind monolayer collapse  
13       is not completely understood, it is well known that compressing monolayers beyond the collapse  
14       pressure causes 2D to 3D transitions by the formation of the lipid aggregates.<sup>49,50</sup> However, these  
15       aggregates, which appear as small, moving islands, were completely stabilized in the presence of  
16       quercetin and tiliroside (**Figure 6b,c**) and the monolayer appearance was still unaltered even  
17       after several hours (data not shown). In the presence of rutin (**Figure 6d**), the monolayer  
18       structure was completely disrupted and all typical DOPC domain structures disappeared. In other  
19       words, introduction of rutin rendered the monolayer appearance entirely smooth and devoid of  
20       lipid islands. One might think that the smooth appearance of the film in the presence of rutin  
21       could be due to the adsorption of the flavonoid. However, if this was the case, a different trend  
22       should have been observed in the RCV plots. Adsorption in RCV traces is characterised by the  
23       suppression of the peaks, such as in the case of silica nanoparticles,<sup>15</sup> but this was not observed.

1  
2  
3 1 Rutin adsorption is therefore an unlikely explanation and the smoothness more probably due to  
4  
5 2 modification of the lipid organisation in the monolayers.  
6  
7

### 8 **SAXS measurements of bilayer flavonoid interactions**

9

10 4 Small angle X-ray scattering (SAXS) experiments were performed to structurally characterize  
11  
12 5 both fully hydrated pure DOPC MLVs and flavonoid loaded vesicles. 6 mol % of flavonoid was  
13  
14 6 chosen for the SAXS study because this concentration was high enough to differentiate between  
15  
16 7 the effects of the different flavonoids but low enough so as not to exceed their solubility limits in  
17  
18 8 the systems. All scattering patterns and their best fits and refined electron density profiles  
19  
20 9 (EDPs) are displayed by solid lines in **Figure 7a** and **Figure 7b**, respectively. EDPs derived  
21  
22 10 from the applied global fitting procedure allowed the determination of structural bilayer  
23  
24 11 parameters summarized in **Figure 8**. These parameters are the (i) lattice spacing,  $d$ , (ii)  
25  
26 12 phosphate-to-phosphate distance within a bilayer, which is also known as head-to-head group  
27  
28 13 thickness,  $d_{HH}$ , (iii) water layer thickness ( $d_w = d - d_{HH}$ ) and (iv) the Caillé parameter,  $\eta$ , from  
29  
30 14 which the mean fluctuations,  $\sigma$ , of the membrane position can deduced according to Equation  
31  
32 15 (1).  
33  
34  
35  
36  
37  
38

39 16 The observed structural behavior of pure DOPC bilayers agrees well with literature findings.<sup>51</sup>  
40  
41 17 While we observed a  $d$ -spacing of 62.5 Å and  $d_{HH}$  of 36.2 Å at room temperature, Nagle et al.,<sup>51</sup>  
42  
43 18 determined values of 63.1 Å and 36.7 Å, respectively, at 30 °C.<sup>51</sup>  
44  
45 19 Remarkably, **Figure 8a** shows that the lattice spacing,  $d$ , do not change significantly by the  
46  
47 20 addition of flavonoids (less than 1% variation), but a closer look at the membrane thickness,  $d_{HH}$   
48  
49 21 (**Figure 8b**), reveals that all compounds studied lead to a membrane thinning effect (up to 5%).  
50  
51 22 Rutin, quercetin and tiliroside decrease the bilayer thickness of DOPC by ~0.45 Å, 0.8 Å and 1.1  
52  
53 23 Å, respectively. Although the thinning in the presence of rutin is not as large, it clearly still  
54  
55  
56  
57  
58  
59  
60

1 requires some interaction of rutin with the bilayers. The only existing study in literature,  
2 characterizing flavonoid- DOPC systems via SAXS was conducted by Raghunathan et al., which  
3 focused only on membrane thickness and for the flavonoids genistein and daidzein only: a  
4 similar membrane thinning effect was revealed in their combined experimental and simulation  
5 study.<sup>8</sup>

6 As shown with **Figure 8c and 8d**, the membrane thinning is accompanied by an increase in the  
7 water layer thickness,  $d_w$ , and a concomitant increase also in the fluctuation parameter,  $\sigma$ , with  
8 tiliroside displaying the largest (6.6 Å; +25%) and rutin the smallest (6.1 Å; +15% ) values,  
9 which compare to positional membrane fluctuations of 5.3 Å in the pure bilayer system. We note  
10 that the fluctuation parameter depends on both the bulk compression modulus and the bending  
11 modulus of the membrane itself.<sup>27</sup> It is necessary to interpret any flavonoid induced membrane  
12 thinning being caused at least in part by an increase in the bilayer fluidity (increased number of  
13 *gauche* conformers in the hydrocarbon chains), since it is well known that this leads to both an  
14 increase in bilayer fluctuations and an increase in bilayer repulsion.<sup>29</sup> Although at 6 mol %  
15 tiliroside displayed the most significant changes when incorporated into bilayers, at lower  
16 concentrations of 1 mol% (data not shown) quercetin was slightly more interactive than  
17 tiliroside, which correlated well with the RCV results discussed in the previous section.

18 The observed structural changes via the X-ray data analysis suggests different penetration  
19 depths of the studied flavonoids. Since rutin increases the membrane fluidity the least (see  
20 **Figure 8d**), a greater molecular overlap with the hydrocarbon chains can be excluded, and we  
21 speculate hydrogen bonding to water and/or polar head groups of the bilayer to be the prominent  
22 interactions, placing rutin mainly in the polar interface of the membrane. In contrast, quercetin  
23 and tiliroside display a more significant increase in the *gauche-trans* conformer ratio in the

1 bilayer (note, the membrane fluctuation are enhanced by about 25%; **Figure 8d**), and hence  
2 might penetrate further into the bilayer. The current view for the localization of the three  
3 compounds correlates well with most other existing studies, which suggest localization of  
4 flavonoids between the boundary of the lipid/water interface and the upper half of the  
5 hydrocarbon chain region.<sup>52,53,54,55,56,57</sup> Notwithstanding this view, some studies suggest that the  
6 flavonoids partition into the hydrophobic region of the membrane.<sup>58,59</sup> An NMR study has  
7 proposed flavonoid localization at the lipid/water interface: the hydroxyl groups have a tendency  
8 to hydrogen bond to the polar head group zone.<sup>54</sup> A FTIR study suggested the same explanation  
9 for quercetin.<sup>55</sup> Movileanu et al.,<sup>53</sup> proposed a pH-dependent insertion of quercetin within  
10 membranes. Quercetin molecules inserted between the polar head groups at alkaline pH, with  
11 deeper localization at acidic pH, due to intercalation of quercetin molecules between the acyl  
12 chains. Rutin-membrane interactions have also been studied via Infrared (IR) spectroscopy. The  
13 frequency shift of hydroxyl and keto groups indicated rutin associated with the polar end of the  
14 phospholipids.<sup>60</sup> In contrast to these findings, Arora et al.,<sup>58</sup> proposed flavonoids and  
15 isoflavonoids tended to insert into the hydrophobic core of membranes, as evidenced by a  
16 significant decrease in membrane fluidity.

## 17 **Conclusions**

18 This study aimed to (i) screen eight flavonoids of systematically varying structure on lipid  
19 monolayers and (ii) identify the structure activity relationship (SAR) based on RCV (iii) link the  
20 SAR to the mechanisms of interactions involved and (iv) employ a widely varying techniques to  
21 support the RCV results and to obtain complementary information on the membrane behavior in  
22 the presence of flavonoids.

1 Electrochemical screening using a DOPC coated Pt/Hg electrode shows a clear structure-  
2 activity relationship in the interaction between flavonoids and DOPC monolayers. Flavonoids  
3 with two coplanar rings were more interactive. On the other hand, flavonoids with two linked  
4 glycoside moieties interacted with DOPC less since these sugar moieties abolish the  
5 hydrophobicity and also render these molecules larger in size. The extent of interactions can be  
6 ranked in the order of quercetin > kaempferol > naringenin > hesperetin > catechin for flavonoid  
7 aglycones and tiliroside > rutin > naringin for flavonoid glycosides.

8 Quercetin and tiliroside interacted to varying degrees with free-standing Langmuir  
9 monolayers at the A-W interface, revealing a clear membrane stabilizing effect on the DOPC  
10 monolayer, whereas rutin showed a different molecular mechanism of action, rendering the  
11 monolayer surface completely smooth and devoid of islands. SAXS analysis of flavonoid loaded  
12 DOPC bilayers showed a clear membrane thinning effect together with an increase in membrane  
13 undulations. Rutin, quercetin and tiliroside thin DOPC by  $\sim 0.45$ ,  $0.8 \text{ \AA}$ , and  $1.1 \text{ \AA}$  at 6 mol %,  
14 respectively. X-ray analysis indicated the location of flavonoids in the bilayer as associated with  
15 polar head groups. The use of a pure DOPC system, one of the most common unsaturated lipids  
16 of the eukaryotic biomembranes, has led to a more detailed and profound analysis of the data  
17 which provides a firm basis for the study of more complex and complete membrane systems in  
18 the future that could include, for example, cholesterol and selected membrane proteins. These  
19 additions, plus the extension to range of different added flavonoid concentrations and  
20 temperatures, is the focus of ongoing work.

## 1 FIGURES

2

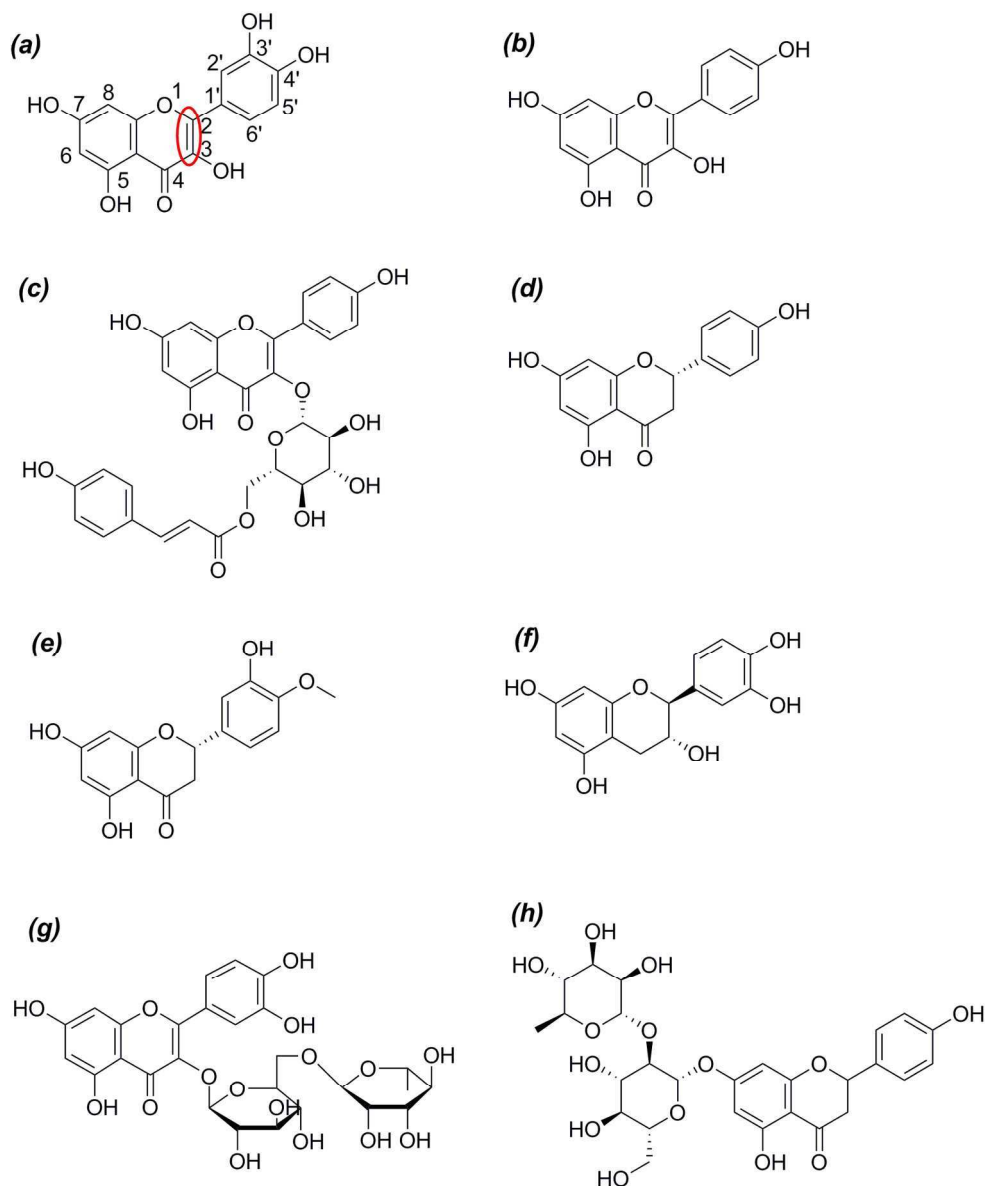


**Figure 1.** Two dimensional structure of compounds used in the current study (a) quercetin dihydrate and numbering pattern for flavonoids (b) kaempferol (c) tiliroside (d) naringenin (e) hesperetin (f) (+)-.catechin (g) rutin trihydrate (h) naringin.

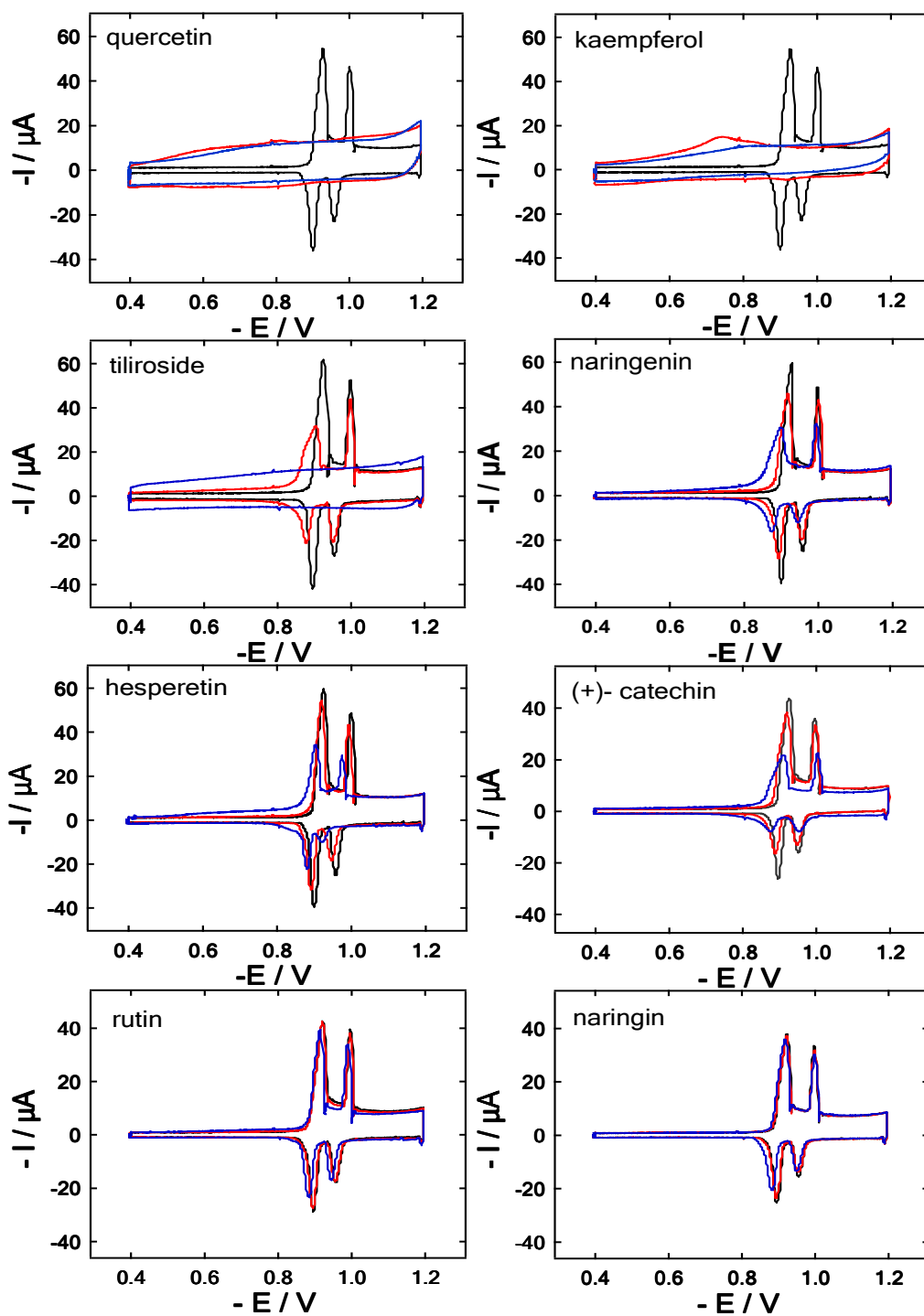


**Figure 2.** RCVs at  $40 \text{ V s}^{-1}$  of a pure DOPC-coated Pt/Hg electrode (black line) in the presence of flavonoids studied at concentrations of  $10 \text{ } \mu\text{mol dm}^{-3}$  (red line) and  $35 \text{ } \mu\text{mol dm}^{-3}$  (blue line) in PBS at pH 7.4.

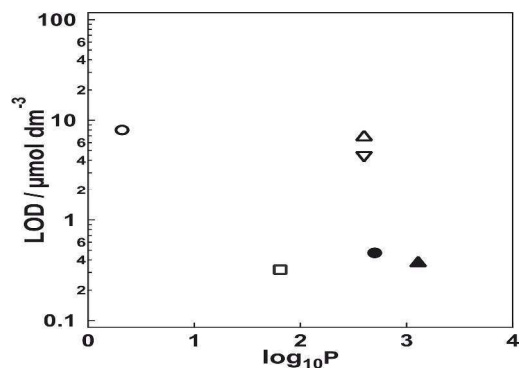


**Figure 3.** Scatter plot to show the compounds' LOD at DOPC-coated Hg electrode in PBS at pH 7.4 vs. their respective log octanol-water partition coefficient ( $\log_{10}P$ ) for following compounds: quercetin (open square), kaempferol (filled triangle), tiliroside (filled circle), naringenin (inverted triangle), hesperetin (open triangle) and (+) - catechin (open circle).

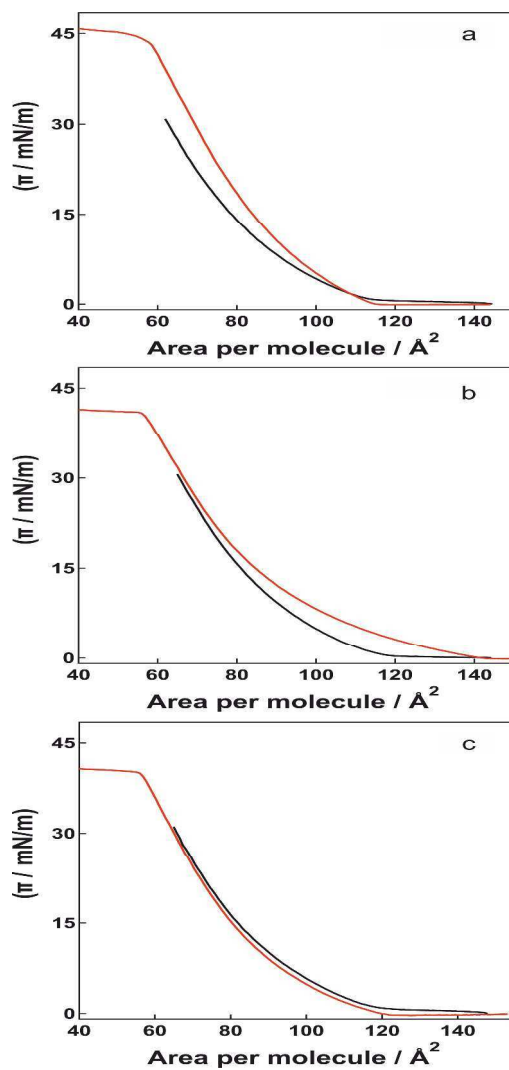


**Figure 4.**  $\pi$ - $A$  isotherms of DOPC monolayer at the air-water interface in the absence (black line) and in the presence of  $10 \mu\text{mol dm}^{-3}$  (a) quercetin, (b) tiliroside and (c) rutin in the subphase (red line).

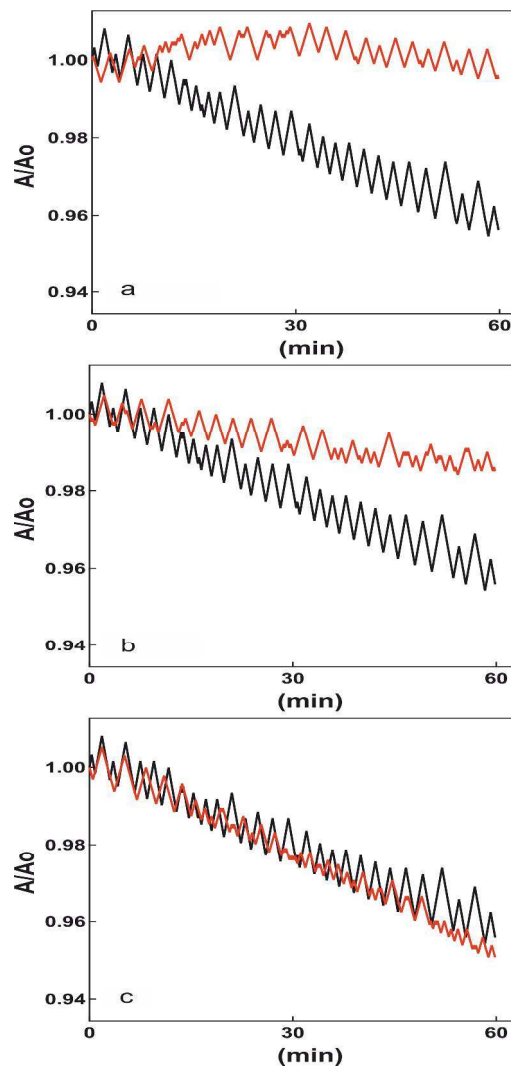
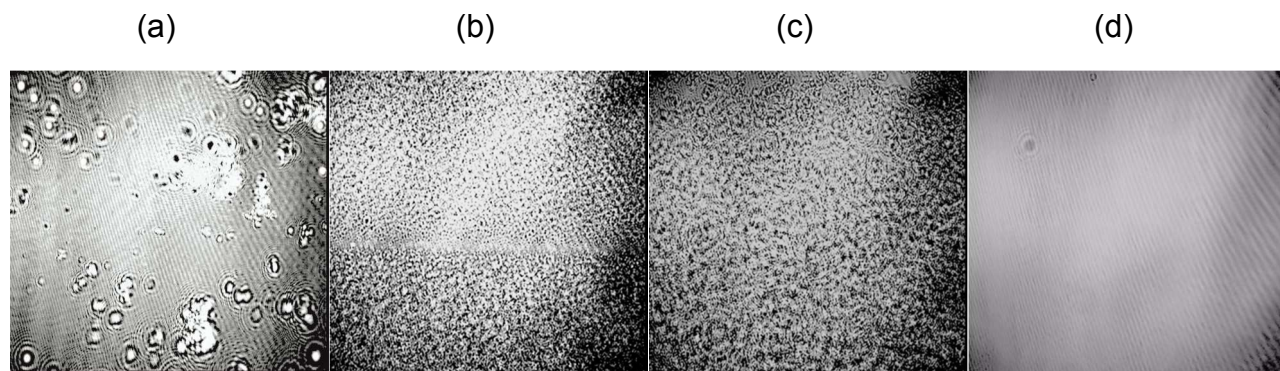


**Figure 5.** Desorption phenomena at constant pressure of  $30 \text{ mN m}^{-1}$  in DOPC monolayers (black line) in the presence of  $10 \mu\text{mol dm}^{-3}$  (a) quercetin, (b) tiliroside and (c) rutin in the subphase (red line).



17  
18  
19  
20  
21  
22  
23  
24  
25  
26  
27  
28  
29  
30  
31  
32  
33  
34  
35  
36  
37  
38  
39  
40  
41  
42  
43  
44  
45  
46  
47  
48  
49  
50  
51  
52  
53  
54  
55  
56  
57  
58  
59  
60

**Figure 6.** BAM images of DOPC monolayers after an hour monolayer collapse (a) pure DOPC monolayer and in the presence of  $10 \mu\text{mol dm}^{-3}$  (b) quercetin (c) tiliroside and (d) rutin in the subphase. (Please note that the numerous closely spaced lines the images are due to optical interference effects that have not been subtracted).

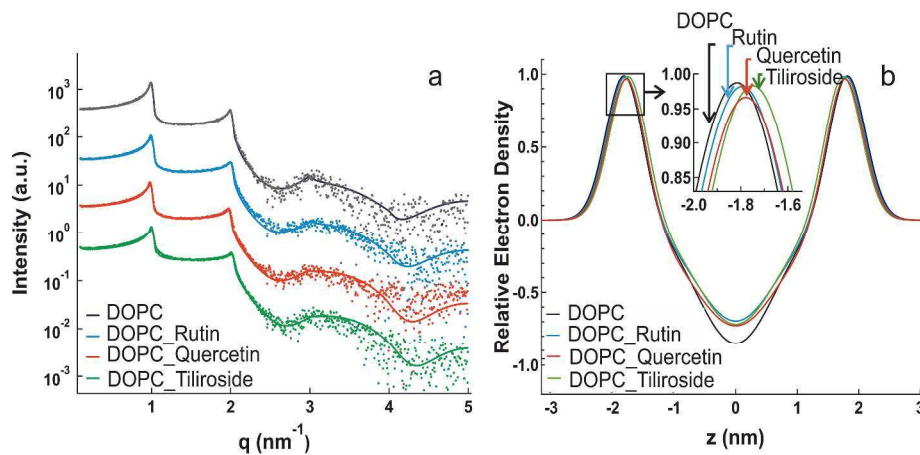


**Figure 7.** (A) Background subtracted SAXS patterns and corresponding fitted curves (solid lines). Data for pure DOPC (gray line) and DOPC with 6 mol. % of rutin (blue line), quercetin (red line) and tiliroside (green line) (B) EDPs of pure DOPC and DOPC-6 mol. % rutin (blue line), DOPC-6 mol. % quercetin (red line), DOPC-6 mol. % tiliroside (green line).

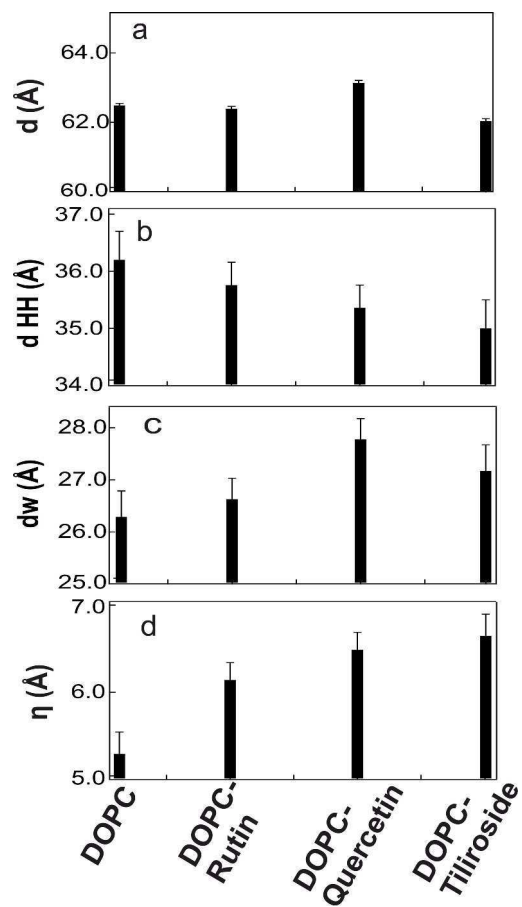


**Figure 8.** Membrane parameters in the presence of 6 mol. % of rutin, quercetin and tiliroside.

**Table 1.** Log<sub>10</sub>*P* values of flavonoids and their LODs using sensing device.

Flavonoids	Experimental log <sub>10</sub> <i>P</i>	LOD / μmol dm <sup>-3</sup>	Configuration	2,3 double bond
<b><u>Flavonol</u></b>				
Quercetin	1.82 <sup>a</sup>	0.32	Planar	Yes
Rutin	-0.87 <sup>b</sup>		Planar	Yes
Kaempferol	3.25 <sup>c</sup>	0.37	Planar	Yes
Tiliroside	2.7 <sup>c</sup>	0.47	Planar	Yes
<b><u>Flavanone</u></b>				
Naringenin	2.70 <sup>c</sup> , 2.60 <sup>a</sup>	4.5	Non-planar	No
Naringin	-0.13 <sup>c</sup>		Non-planar	No
Hesperetin	2.60 <sup>d</sup>	6.8	Non-planar	No
<b><u>Flavan-3-ols</u></b>				
Catechin	0.32 <sup>e</sup>	8	Non-planar	No

<sup>a</sup> Experimental log<sub>10</sub>*P* from Rothwell et al<sup>61</sup>. <sup>b</sup> log<sub>10</sub> *P* from *DrugBank*<sup>62</sup>. <sup>c</sup> Experimental log<sub>10</sub>*P* from Luo et al<sup>63</sup>. <sup>d</sup> Experimental log<sub>10</sub>*P* from Cooper et al<sup>64</sup>. <sup>e</sup> Experimental log<sub>10</sub>*P* from Shibusawa et al<sup>65</sup>.

1  
2  
3 Corresponding Author  
4  
5

6 \*E-mail: [b.s.murray@leeds.ac.uk](mailto:b.s.murray@leeds.ac.uk) (B. S. Murray)  
7  
8

9  
10 **ACKNOWLEDGMENT**  
11

12 The authors are grateful to Dr. Alexandre Vakurov, Dr. Shahrzad Mohamadi and Dr. Mahmood  
13 Akhtar for their experimental and technical support.  
14  
15  
16  
17  
18  
19  
20  
21  
22  
23  
24  
25  
26  
27  
28  
29  
30  
31  
32  
33  
34  
35  
36  
37  
38  
39  
40  
41  
42  
43  
44  
45  
46  
47  
48  
49  
50  
51  
52  
53  
54  
55  
56  
57  
58  
59  
60

## REFERENCES

1. Andersen, O. M.; Markham, K. R., *Flavonoids : Chemistry, Biochemistry and Applications*. New ed.; CRC: Boca Raton, Fla. ; London, 2006; p 1237 p.
2. Rice-Evans, C.; Packer, L., *Flavonoids in health and disease*. 2nd. ed.; Marcel Dekker: New York, 2003; p xiii, 467 p.
3. Luca, V. S.; Miron, A.; Aprotosoiaie, A. C., The antigenotoxic potential of dietary flavonoids. *Phytochemistry Reviews* **2016**, 1-35.
4. Weng, Z.; Zhang, B.; Asadi, S.; Sismanopoulos, N.; Butcher, A.; Fu, X.; Katsarou-Katsari, A.; Antoniou, C.; Theoharides, T. C., Quercetin is more effective than cromolyn in blocking human mast cell cytokine release and inhibits contact dermatitis and photosensitivity in humans. *Plos One* **2012**, 7 (3), e33805.
5. Horcajada, M.-N.; Sanchez, C.; Scalfò, F. M.; Drion, P.; Comblain, F.; Taralla, S.; Donneau, A.-F.; Offord, E.; Henrotin, Y., Oleuropein or rutin consumption decreases the spontaneous development of osteoarthritis in the Hartley guinea pig. *Osteoarthritis and Cartilage* **2015**, 23 (1), 94-102.
6. Tsuchiya, H., Membrane Interactions of Phytochemicals as Their Molecular Mechanism Applicable to the Discovery of Drug Leads from Plants. *Molecules* **2015**, 20 (10), 18923-18966.
7. Ingólfsson, H. I.; Thakur, P.; Herold, K. F.; Hobart, E. A.; Ramsey, N. B.; Periole, X.; de Jong, D. H.; Zwama, M.; Yilmaz, D.; Hall, K., Phytochemicals perturb membranes and promiscuously alter protein function. *ACS chemical biology* **2014**, 9 (8), 1788-1798.
8. Raghunathan, M.; Zubovski, Y.; Venable, R. M.; Pastor, R. W.; Nagle, J. F.; Tristram-Nagle, S., Structure and elasticity of lipid membranes with genistein and daidzein bioflavonoids using X-ray scattering and MD simulations. *The Journal of Physical Chemistry B* **2012**, 116 (13), 3918-3927.
9. Peetla, C.; Stine, A.; Labhassetwar, V., Biophysical interactions with model lipid membranes: applications in drug discovery and drug delivery. *Molecular pharmaceutics* **2009**, 6 (5), 1264-1276.
10. Pignatello, R.; Musumeci, T.; Basile, L.; Carbone, C.; Puglisi, G., Biomembrane models and drug-biomembrane interaction studies: Involvement in drug design and development. *Journal of Pharmacy And Bioallied Sciences* **2011**, 3 (1), 4.
11. Selvaraj, S.; Krishnaswamy, S.; Devashya, V.; Sethuraman, S.; Krishnan, U. M., Influence of membrane lipid composition on flavonoid–membrane interactions: Implications on their biological activity. *Progress in Lipid Research* **2015**, 58 (0), 1-13.
12. Coldrick, Z.; Steenson, P.; Millner, P.; Davies, M.; Nelson, A., Phospholipid monolayer coated microfabricated electrodes to model the interaction of molecules with biomembranes. *Electrochim Acta* **2009**, 54 (22), 4954-4962.
13. Vakurov, A.; Drummond-Brydson, R.; Ugwumsinachi, O.; Nelson, A., Significance of particle size and charge capacity in TiO<sub>2</sub> nanoparticle-lipid interactions. *J Colloid Interf Sci* **2016**, 473, 75-83.
14. Stoodley, R.; Bizzotto, D., Epi-fluorescence microscopic characterization of potential-induced changes in a DOPC monolayer on a Hg drop. *Analyst* **2003**, 128 (6), 552-561.

15. Vakurov, A.; Brydson, R.; Nelson, A., Electrochemical modeling of the silica nanoparticle–biomembrane interaction. *Langmuir* **2011**, *28* (2), 1246-1255.
16. Ter Minassian-Saraga, L., Recent work on spread monolayers, adsorption and desorption. *Journal of Colloid Science* **1956**, *11* (4), 398-418.
17. Nelson, A., Electrochemistry of mercury supported phospholipid monolayers and bilayers. *Current Opinion in Colloid & Interface Science* **2010**, *15* (6), 455-466.
18. Ding, W.; Palaiokostas, M.; Wang, W.; Orsi, M., Effects of Lipid Composition on Bilayer Membranes Quantified by All-Atom Molecular Dynamics. *The Journal of Physical Chemistry B* **2015**.
19. Valério, J.; Lameiro, M. H.; Funari, S. S.; Moreno, M. J.; Melo, E., Temperature effect on the bilayer stacking in multilamellar lipid vesicles. *The Journal of Physical Chemistry B* **2011**, *116* (1), 168-178.
20. Williamson, G.; Manach, C., Bioavailability and bioefficacy of polyphenols in humans. II. Review of 93 intervention studies. *The American journal of clinical nutrition* **2005**, *81* (1), 243S-255S.
21. Murray, B. S.; Nelson, P. V., A novel langmuir trough for equilibrium and dynamic measurements on air-water and oil-water monolayers. *Langmuir* **1996**, *12* (25), 5973-5976.
22. Janmey, P.; Kinnunen, P., Biophysical properties of lipids and dynamic membranes. *Trends in cell biology* **2006**, *16* (10), 538-546.
23. Garofalakis, G.; Murray, B. S., Surface pressure isotherms, dilatational rheology, and Brewster angle microscopy of insoluble monolayers of sugar monoesters. *Langmuir* **2002**, *18* (12), 4765-4774.
24. Xu, R.; Dickinson, E.; Murray, B. S., Morphological changes in adsorbed protein films at the air-water interface subjected to large area variations, as observed by Brewster angle microscopy. *Langmuir* **2007**, *23* (9), 5005-5013.
25. Drasler, B.; Drobne, D.; Sadeghpour, A.; Rappolt, M., Fullerene up-take alters bilayer structure and elasticity: A small angle X-ray study. *Chemistry and physics of lipids* **2015**, *188*, 46-53.
26. Patil-Sen, Y.; Sadeghpour, A.; Rappolt, M.; Kulkarni, C. V., Facile preparation of internally self-assembled lipid particles stabilized by carbon nanotubes. *JoVE (Journal of Visualized Experiments)* **2016**, (108), e53489-e53489.
27. Pabst, G.; Rappolt, M.; Amenitsch, H.; Laggner, P., Structural information from multilamellar liposomes at full hydration: full q-range fitting with high quality x-ray data. *Physical Review E* **2000**, *62* (3), 4000.
28. Pabst, G.; Katsaras, J.; Raghunathan, V. A.; Rappolt, M., Structure and interactions in the anomalous swelling regime of phospholipid bilayers. *Langmuir* **2003**, *19* (5), 1716-1722.
29. Rappolt, M.; Pabst, G., Flexibility and structure of fluid bilayer interfaces. *Structure and Dynamics of Membranous Interfaces* **2008**, 45-81.
30. PABST, G., Global properties of biomimetic membranes: perspectives on molecular features. *Biophysical Reviews and Letters* **2006**, *1* (01), 57-84.
31. Rappolt, M., Bilayer thickness estimations with “poor” diffraction data. *J Appl Phys* **2010**, *107* (8), 084701.
32. Ormategui, N.; Zhang, S.; Loinaz, I.; Brydson, R.; Nelson, A.; Vakurov, A., Interaction of poly(N-isopropylacrylamide) (pNIPAM) based nanoparticles and their linear polymer precursor with phospholipid membrane models. *Bioelectrochemistry* **2012**, *87*, 211-219.

- 1  
2  
3 33. Mohamadi, S.; Tate, D. J.; Vakurov, A.; Nelson, A., Electrochemical screening of  
4 biomembrane-active compounds in water. *Analytica chimica acta* **2014**, *813*, 83-89.
- 5 34. van Dijk, C.; Driessen, A. J. M.; Recourt, K., The uncoupling efficiency and affinity of  
6 flavonoids for vesicles. *Biochemical Pharmacology* **2000**, *60* (11), 1593-1600.
- 7 35. Ferriola, P. C.; Cody, V.; Middleton Jr, E., Protein kinase C inhibition by plant  
8 flavonoids: Kinetic mechanisms and structure-activity relationships. *Biochemical Pharmacology*  
9 **1989**, *38* (10), 1617-1624.
- 10 36. Saija, A.; Scalse, M.; Lanza, M.; Marzullo, D.; Bonina, F.; Castelli, F., Flavonoids as  
11 antioxidant agents: Importance of their interaction with biomembranes. *Free Radical Biology*  
12 *and Medicine* **1995**, *19* (4), 481-486.
- 13 37. Londoño-Londoño, J.; Lima, V. R. D.; Jaramillo, C.; Creczynski-pasa, T., Hesperidin and  
14 hesperetin membrane interaction: Understanding the role of 7-O-glycoside moiety in flavonoids.  
15 *Arch Biochem Biophys* **2010**, *499* (1-2), 6-16.
- 16 38. Izumi, T.; Piskula, M. K.; Osawa, S.; Obata, A.; Tobe, K.; Saito, M.; Kataoka, S.;  
17 Kubota, Y.; Kikuchi, M., Soy isoflavone aglycones are absorbed faster and in higher amounts  
18 than their glucosides in humans. *The Journal of nutrition* **2000**, *130* (7), 1695-1699.
- 19 39. Ferreira, J. V. N.; Grecco, S. d. S.; Lago, J. H. G.; Caseli, L., Ultrathin films of lipids to  
20 investigate the action of a flavonoid with cell membrane models. *Materials Science and*  
21 *Engineering: C* **2015**, *48* (0), 112-117.
- 22 40. Schmidt, T. F.; Caseli, L.; Oliveira Jr, O. N.; Itri, R., Binding of Methylene Blue onto  
23 Langmuir Monolayers Representing Cell Membranes May Explain Its Efficiency as  
24 Photosensitizer in Photodynamic Therapy. *Langmuir* **2015**, *31* (14), 4205-4212.
- 25 41. Walker, I.; Gorman, S. A.; Cox, R. D.; Vernon, D. I.; Griffiths, J.; Brown, S. B., A  
26 comparative analysis of phenothiazinium salts for the photosensitisation of murine fibrosarcoma  
27 (RIF-1) cells in vitro. *Photochemical & Photobiological Sciences* **2004**, *3* (7), 653-659.
- 28 42. Gaines, G. L., Insoluble monolayers at liquid-gas interfaces. **1966**.
- 29 43. Niño, M. R. R.; Lucero, A.; Patino, J. M. R., Relaxation phenomena in phospholipid  
30 monolayers at the air-water interface. *Colloids and Surfaces A: Physicochemical and*  
31 *Engineering Aspects* **2008**, *320* (1), 260-270.
- 32 44. Sinha, R.; Gadhwal, M.; Joshi, U.; Srivastava, S.; Govil, G., Modifying effect of  
33 quercetin on model biomembranes: studied by molecular dynamic simulation, DSC and NMR.  
34 *Int J Curr Pharm Res* **2012**, *4*, 70-9.
- 35 45. Kurkin, V.; Ryzhov, V.; Biryukova, O.; Mel'nikova, N.; Selekhev, V., Interaction of  
36 milk-thistle-fruit flavanones with Langmuir monolayers of lecithin and bilayers of liposomes.  
37 *Pharmaceutical chemistry journal* **2009**, *43* (2), 101-109.
- 38 46. Lucero, A.; Rodríguez Niño, M.; Gunning, A.; Morris, V.; Wilde, P.; Rodríguez Patino,  
39 J., Effect of hydrocarbon chain and pH on structural and topographical characteristics of  
40 phospholipid monolayers. *The Journal of Physical Chemistry B* **2008**, *112* (25), 7651-7661.
- 41 47. Patino, J. M. R.; Caro, A. L.; Niño, M. R. R.; Mackie, A. R.; Gunning, A. P.; Morris, V.  
42 J., Some implications of nanoscience in food dispersion formulations containing phospholipids  
43 as emulsifiers. *Food chemistry* **2007**, *102* (2), 532-541.
- 44 48. Saccani, J.; Castano, S.; Beaurain, F.; Laguerre, M.; Desbat, B., Stabilization of  
45 phospholipid multilayers at the air-water interface by compression beyond the collapse: a BAM,  
46 PM-IRRAS, and molecular dynamics study. *Langmuir* **2004**, *20* (21), 9190-9197.
- 47 49. Lee, K. Y. C., Collapse mechanisms of Langmuir monolayers. *Annu. Rev. Phys. Chem.*  
48 **2008**, *59*, 771-791.
- 49  
50  
51  
52  
53  
54  
55  
56  
57  
58  
59  
60

- 1  
2  
3  
4  
5  
6  
7  
8  
9  
10  
11  
12  
13  
14  
15  
16  
17  
18  
19  
20  
21  
22  
23  
24  
25  
26  
27  
28  
29  
30  
31  
32  
33  
34  
35  
36  
37  
38  
39  
40  
41  
42  
43  
44  
45  
46  
47  
48  
49  
50  
51  
52  
53  
54  
55  
56  
57  
58  
59  
60
50. Ybert, C.; Lu, W.; Möller, G.; Knobler, C. M., Collapse of a monolayer by three mechanisms. *The Journal of Physical Chemistry B* **2002**, *106* (8), 2004-2008.
  51. Nagle, J. F.; Tristram-Nagle, S., Structure of lipid bilayers. *Biochimica et Biophysica Acta (BBA)-Reviews on Biomembranes* **2000**, *1469* (3), 159-195.
  52. Ollila, F.; Halling, K.; Vuorela, P.; Vuorela, H.; Slotte, J. P., Characterization of Flavonoid–Biomembrane Interactions. *Arch Biochem Biophys* **2002**, *399* (1), 103-108.
  53. Movileanu, L.; Neagoe, I.; Flonta, M. L., Interaction of the antioxidant flavonoid quercetin with planar lipid bilayers. *Int J Pharm* **2000**, *205* (1–2), 135-146.
  54. Scheidt, H. A.; Pampel, A.; Nissler, L.; Gebhardt, R.; Huster, D., Investigation of the membrane localization and distribution of flavonoids by high-resolution magic angle spinning NMR spectroscopy. *Biochimica et Biophysica Acta (BBA)-Biomembranes* **2004**, *1663* (1), 97-107.
  55. Pawlikowska-Pawłęga, B.; Dziubińska, H.; Król, E.; Trębacz, K.; Jarosz-Wilkolazka, A.; Paduch, R.; Gawron, A.; Gruszecki, W. I., Characteristics of quercetin interactions with liposomal and vacuolar membranes. *Biochimica et Biophysica Acta (BBA) - Biomembranes* **2014**, *1838* (1, Part B), 254-265.
  56. Košinová, P. n.; Berka, K.; Wykes, M.; Otyepka, M.; Trouillas, P., Positioning of antioxidant quercetin and its metabolites in lipid bilayer membranes: implication for their lipid-peroxidation inhibition. *The Journal of Physical Chemistry B* **2012**, *116* (4), 1309-1318.
  57. Chulkov, E. G.; Ostroumova, O. S., Phloretin modulates the rate of channel formation by polyenes. *Biochimica et Biophysica Acta (BBA)-Biomembranes* **2016**, *1858* (2), 289-294.
  58. Arora, A.; Byrem, T. M.; Nair, M. G.; Strasburg, G. M., Modulation of Liposomal Membrane Fluidity by Flavonoids and Isoflavonoids. *Arch Biochem Biophys* **2000**, *373* (1), 102-109.
  59. Tedeschi, A.; D'Errico, G.; Lauro, M. R.; Sansone, F.; Di Marino, S.; D'Ursi, A. M.; Aquino, R. P., Effect of flavonoids on the A $\beta$ (25-35)-phospholipid bilayers interaction. *European Journal of Medicinal Chemistry* **2010**, *45* (9), 3998-4003.
  60. Singh, D.; SM Rawat, M.; Semalty, A.; Semalty, M., Rutin-phospholipid complex: an innovative technique in novel drug delivery system-NDDS. *Current drug delivery* **2012**, *9* (3), 305-314.
  61. Rothwell, J. A.; Day, A. J.; Morgan, M. R., Experimental determination of octanol-water partition coefficients of quercetin and related flavonoids. *J Agr Food Chem* **2005**, *53* (11), 4355-4360.
  62. Wishart, D. S.; Knox, C.; Guo, A. C.; Shrivastava, S.; Hassanali, M.; Stothard, P.; Chang, Z.; Woolsey, J., DrugBank: a comprehensive resource for in silico drug discovery and exploration. *Nucleic Acids Research* **2006**, *34* (Database issue), D668-D672.
  63. Luo, Z. J.; Murray, B. S.; Yusoff, A.; Morgan, M. R. A.; Povey, M. J. W.; Day, A. J., Particle-Stabilizing Effects of Flavonoids at the Oil-Water Interface. *J Agr Food Chem* **2011**, *59* (6), 2636-2645.
  64. Cooper, D. A.; Webb, D. R.; Peters, J. C., Evaluation of the potential for olestra to affect the availability of dietary phytochemicals. *The Journal of nutrition* **1997**, *127* (8), 1699S-1709S.
  65. Shibusawa, Y.; Shoji, A.; Yanagida, A.; Shindo, H.; Tagashira, M.; Ikeda, M.; Ito, Y., Determination of log Po/w for catechins and their isomers, oligomers, and other organic compounds by stationary phase controlled high-speed countercurrent chromatography. *Journal of liquid chromatography & related technologies* **2005**, *28* (17), 2819-2837.

1  
2  
3  
4  
5  
6  
7  
8  
9  
10  
11  
12  
13  
14  
15  
16  
17  
18  
19  
20  
21  
22  
23  
24  
25  
26  
27  
28  
29  
30  
31  
32  
33  
34  
35  
36  
37  
38  
39  
40  
41  
42  
43  
44  
45  
46  
47  
48  
49  
50  
51  
52  
53  
54  
55  
56  
57  
58  
59  
60

1  
2  
3 Table of Contents Graphic:  
4  
5  
6  
7  
8  
9

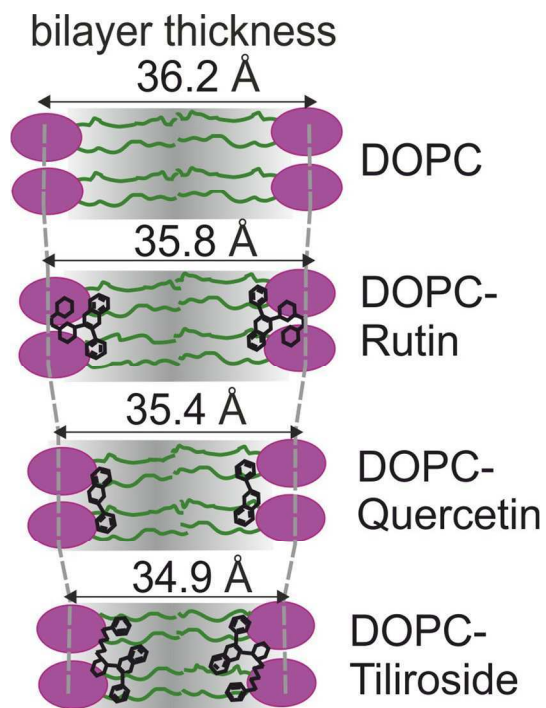


Table of Contents Graphic: Solubilization of flavonoids into DOPC bilayers

